An Atlas of LAMOST Low-Resolution Spectra of Chemically Peculiar Stars

Stefan Hümmerich
(email: ernham@rz-online.de)

August 23, 2021

Contents

1 Introduction

The present work was conceived while I was familiarizing myself with the appearance of different groups of chemically peculiar (CP) stars in spectra from the Large Sky Area Multi-Object Fiber Spectroscopic Telescope (LAMOST). While there are many excellent resources on spectral classification and CP stars, more often than not, I found myself wishing for a concise source that provides an overview over the different classes of CP stars at LAMOST resolution. Addressing this gap, the here presented atlas showcases representative LAMOST spectra of the most important classes of upper main-sequence CP stars and shortly discusses their spectral peculiarities and the more common pitfalls encountered in the classification of these objects, with the intention of facilitating the approach to the study of these interesting stars. It is perhaps best viewed as a supplement to the Digital Spectral Classification Atlas of Richard O. Gray, whom I thank for his constructive criticism and the hosting of this document. As methodological basis underlying this work, I would like to highlight Stellar Spectral Classification, the classic textbook by R. O. Gray and Chris Corbally (Gray and Corbally 2009), and the series of papers dealing with precision classification of B, A, and F stars by R. O. Gray and Robert F. Garrison (Gray and Garrison 1987, 1989a,b; Garrison and Gray 1994).

For convenience, all spectra presented in the atlas are provided for download in the Appendix – in original LAMOST format as well as in rectified and normalized flux, which is the basis for all figures depicted herein. If any part of this atlas is beneficial to your research or teaching practice, please feel free to make use of the information provided herein as suits your needs. However, an appropriate acknowledgment of the LAMOST project is requested, and an acknowlegdement of this document encouraged. If nothing else, I hope that this atlas may serve to illustrate the beauty and variety of CP star spectra, which, to my mind, are a most fascinating field of study. Please note also that this is a work in progress that will be revised and enlarged with further chapters from time to time. All changes from one version to the next will be documented. Finally, all spectral classifications provided herein are my own; thus, any errors or inaccuracies connected with them are entirely my own, too.

1.1 Chemically Peculiar Stars of the Upper Main Sequence

There are many excellent reviews on CP stars, and it is not the intention of the present work to provide a comprehensive overview. In a nutshell, CP stars are characterized by certain spectral peculiarities, generally unusually strong or weak absorption lines of certain elements or sets of elements. Further information on CP stars may be gathered from the overviews provided for example by Preston (1974), Wolff (1983), and Gray and Corbally (2009), and the references therein.

The present work is concerned with the CP stars of the upper main sequence (spectral types early B to early F) – that is, the metallic-line or Am stars (also termed CP1 stars), the magnetic Ap (CP2) stars, the mercury-manganese (HgMn/CP3) stars, and the He-weak (CP4) stars (Preston 1974) – and their classification in the traditional blue-violet optical region ($\lambda\lambda 3800{-}4600$ Å). Also commented on are the groups of the He-rich stars and the metal-weak λ Bootis stars. Main emphasis has been placed on the Ap stars. Throughout the text, the coordinate-based identifiers given refer to the LAMOST identifiers (LAMOST JHHMMSS.ss+DDMMSS.s). Alternative identifiers, and the sources from which the CP stars have been gleaned, are presented in the Appendix. The standard spectra used in this work were taken from the *libr18* collections of standard star spectra available from R. O. Gray's MKCLASS website[1]. Synthetic spectra were calculated using the SPECTRUM

[1] http://www.appstate.edu/~grayro/mkclass/

code[2] (Gray and Corbally 1994) and ATLAS9 model atmospheres (Castelli and Kurucz 2003).

It is important to note that at the resolution of the LAMOST low-resolution spectra, all lines and blends used in this study are, to some extent, blended with other absorption lines. Nevertheless, the specified elements generally constitute the main contributors to these blends in the investigated groups of CP stars.

1.2 The Large Sky Area Multi-Object Fiber Spectroscopic Telescope (LAMOST)

The LAMOST telescope is located at the Xinglong Observatory in Beijing, China. It is a large-aperture (4m) reflecting Schmidt telescope that commands a field of view of 5° and is able to take 4000 spectra in a single exposure down to a limiting magnitude of $r \sim 19$ mag. The LAMOST low-resolution spectra have a spectral resolution of $R = 1800$ and cover the wavelength range from 3700 to 9000 Å. LAMOST is dedicated to a spectral survey of the entire available northern sky. Boasting more than 11 million spectra already, the LAMOST archive constitutes a most valuable resource. LAMOST data products are released to the public in consecutive data releases and can be accessed via the LAMOST spectral archive.[3] More information on LAMOST is provided for example in Zhao et al. (2012) and Cui et al. (2012). All spectra shown in this atlas were taken from LAMOST Data Release 4 (Luo et al. 2018).

[2] http://www.appstate.edu/~grayro/spectrum/spectrum.html
[3] http://www.lamost.org

2 The Am stars

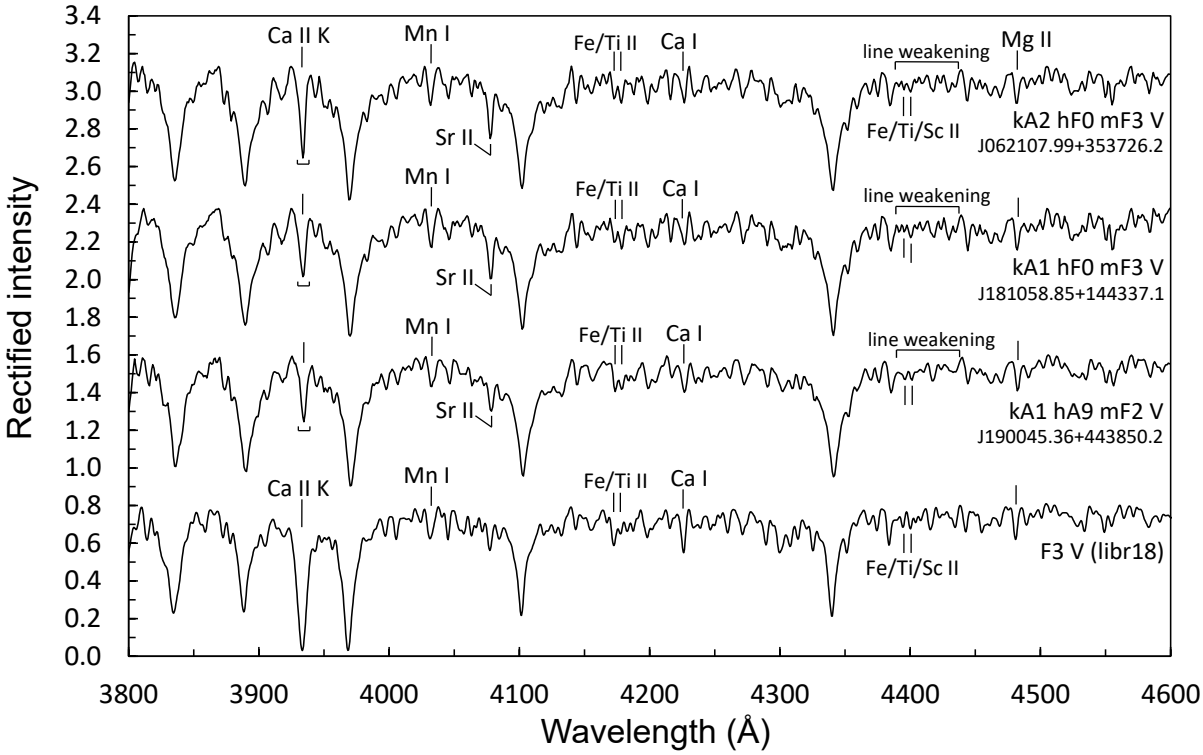

Figure 1: Three representative Am stars, compared with the spectrum of the F3 V standard HR 1279, which has been taken from the *libr18* collection of standard spectra and smoothed to approximately match the LAMOST resolution. While the metallic-line spectra of the Am stars appear slightly later than their hydrogen-line types, their Ca II K lines are clearly weak and best matched by that of A1 V and A2 V standards, respectively. Note also the peculiarly strong Sr λ4077 lines and the weakening of the absorption lines in the $\lambda\lambda$4395−4400 region.

The Am/CP1 stars are A- and early F-type stars characterized by significant underabundances of Ca and Sc and general overabundances of iron-peak and heavier elements. This manifests itself in weak Ca II K lines and pronounced metallic-line spectra in these objects, which, by definition, show a discrepancy between the spectral types derived from the strength of the Ca II K line and the metallic lines by at least five spectral subclasses. Stars in which the difference is less pronounced are sometimes referred to as 'marginal-' or 'proto-'Am stars (e.g. Morgan et al. 1978). Next to a weak Ca II K line, Am stars also have weak Ca I λ4226 lines, and there is a noticeable weakening of the absorption lines in the $\lambda\lambda$4395−4400 region, which contain significant contributions from Sc II. In the classification of Am stars, the spectral types derived from the Ca II K line (the k-line type), the hydrogen lines (the h-line type), and the strength of the metallic lines (the m-line type) are indicated (Fig. 1). Care needs to be taken in the luminosity classification of these objects, as many of the lines traditionally used in this process are either enhanced (such as Sr II λ4077 and Fe/Ti II $\lambda\lambda$4172−9) or weakened (such as λ4417). At LAMOST resolution, the most conspicuous feature of Am stars is the readily visible discrepancy between the Ca II K line strength and the pronounced metallic-line spectrum. The classifier needs to be aware, however, that the spectra of cool Ap stars often share these characteristics (cf. Sect. 3.4), and, on first glance, may look similar.

3 The Ap stars

Ap/CP2 stars exhibit a bewildering amount of diversity in their spectra, and some of the most peculiar objects known, like Przybylski's star (Przybylski 1961), belong to this group. Whereas Am stars show general overabundances of iron-peak and heavier elements, only selected elements are enhanced in Ap stars. They are encountered in the large temperature range of $7000\,\mathrm{K} \leq T_{eff} \leq 16000\,\mathrm{K}$ and present very different spectra at the hot and cool end of their distribution.

Many classification systems for Ap stars have been proposed in the literature, and, at high resolution, it is quite possible that no two Ap star spectra look the same. At LAMOST resolution, the present author has found it useful to at least distinguish between the hot Si stars, the SiCrEu stars (stars that show other peculiarities, mostly Cr and Eu, in addition to strongly enhanced Si II lines), the EuCrSr stars (stars whose spectra are mostly dominated by enhanced Eu II, Cr II and Sr II lines), and the cool SrCrEu stars, all of which are dealt with in more detail in the following sections. Note that these terms are only guidelines and not used mandatorily in the sense that the indicated peculiarities are necessarily present in every single specimen of a particular group. There are, for example, SiCrEu stars that do not exhibit any appreciable Eu II features (cf. the spectrum of the J195251.15+403621.4 shown in Fig. 4). Even at this resolution, the diversity of Ap star spectra is intriguing and the displayed phenomena are complex. Therefore, "[...] any classification scheme is open to criticism, in the sense that exceptions can always be found." (Jaschek and Jaschek 1987, p. 176). Furthermore, Ap stars are spectrum variables, which heightens their interest but which should always be kept in mind when dealing with these objects.

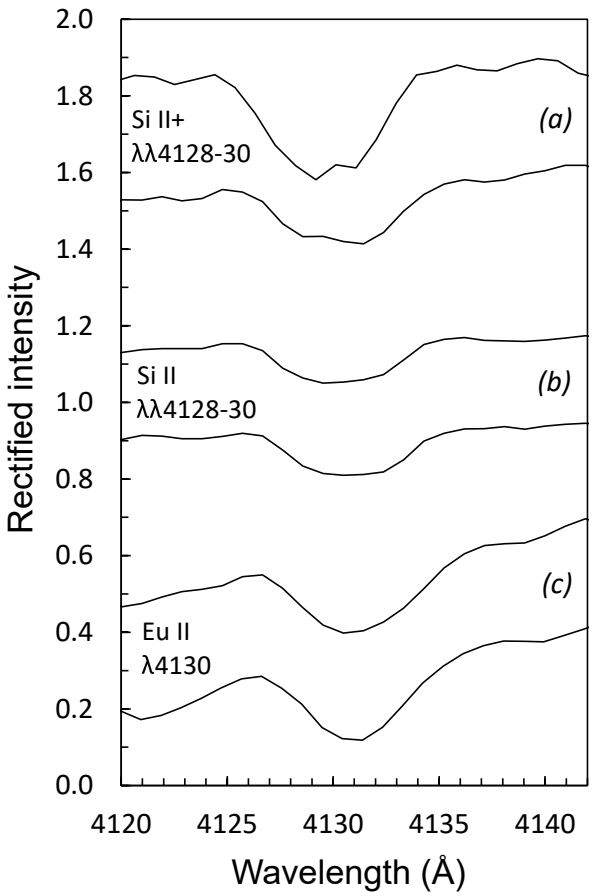

Figure 2: Different morphology of the λ4130 blend at LAMOST resolution.

When classifying Ap star spectra at low resolution, "[..p]erhaps the most deceptive feature is the presence of a strong, broad blend centered near λ4130." (Gray and Corbally 2009, p. 187). In the hotter Ap stars, this blend is generally due to the Si II $\lambda\lambda$4128−30 doublet, while in the cooler stars, it is primarily caused by a strong Eu II λ4130 line. At LAMOST resolution, on close inspection, the former feature may appear partly resolved in the more narrow-lined stars (Fig. 2a) but generally shows a flat-bottomed morphology (Fig. 2b), while the latter feature appears more rounded (Fig. 2c). Nevertheless, it is necessary to check additional Si II or Eu II lines to judge the contributions of these ions to the observed λ4130 blend. The spectra shown belong, from top to bottom, to (a) the SiCrEu stars J052043.33+380212.5 and J001345.60+562953.5, (b) the hot Si stars J003312.88+543141.3 and J060809.53+240945.0, and (c) the cool SrCrEu stars J062449.08+190854.0 and J062221.82+595613.0, which are all dealt with in more detail in the following sections.

In a similar manner, care needs to be taken in the interpretation of the strong λ4077 line, which is a characteristic feature of especially the cooler Ap stars. It may contain contributions from different ions such as Si II λ4076, Sr II λ4077, and Cr II λ4077, whose contributions need to be judged from other relevant lines of these ions. A good overview on prominent lines in the blue-violet spectra of Ap stars is provided in Table 5.1 of Gray and Corbally (2009).

Apart from that, the classifier needs to be aware that certain traditional classification criteria may not yield trustworthy results for Ap stars. In particular, it is important to keep in mind the following points.

- Ap stars tend to show peculiarly weak or strong Ca II K lines. A temperature type based on the strength of the Ca II K line is therefore unreliable.
- The atmospheres of many Ap stars are noticeably deficient in He, which results in weak He I lines in their spectra.
- The metallic-line spectra of Ap stars are so peculiar that the applicability of many lines traditionally used in temperature or luminosity classification is severely compromised, as these lines may appear peculiarly weak or strong.

Because of this, the temperature and luminosity type of an Ap star is best based on the appearance of the hydrogen-line profile (Gray and Corbally 2009). This, however, may also show certain peculiarities, which are discussed in more detail in Sect. 3.5. In the following sections, We have determined spectral types based on the CaiiK linestrength (the k-line type) and the hydrogen-line profile (the h-linetype) (Osawa 1965).

3.1 The hot Si stars

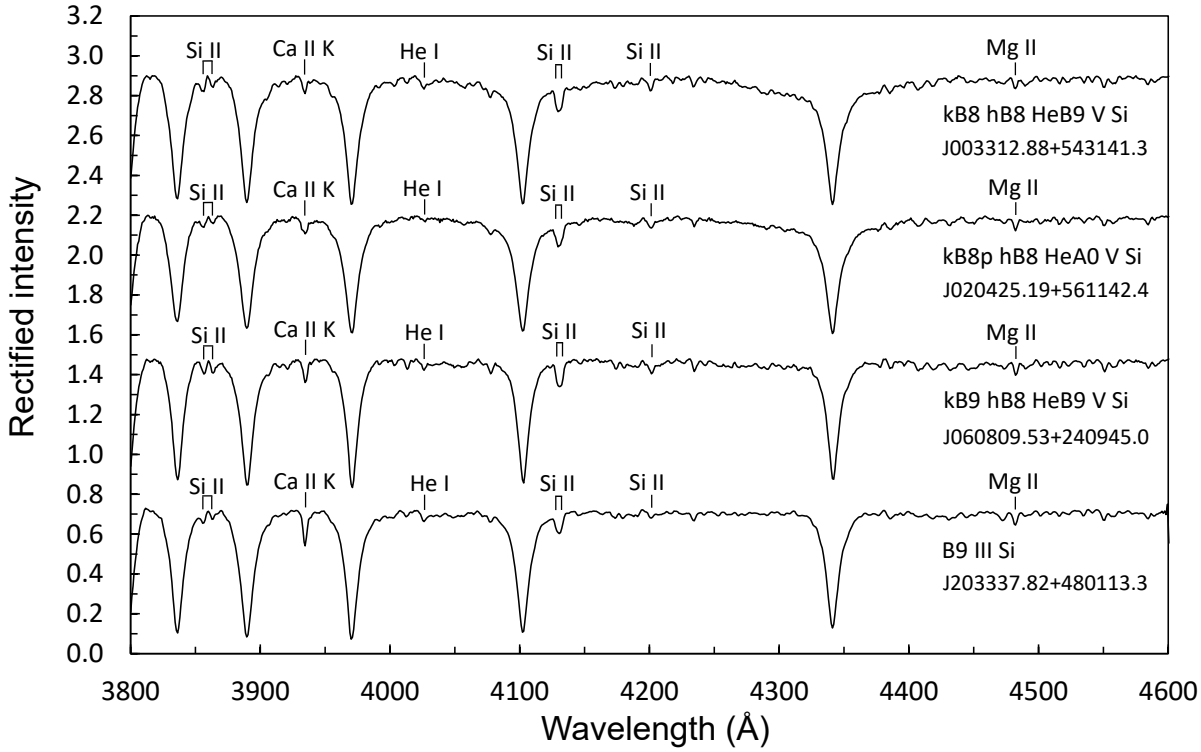

Figure 3: Four representative hot Si Ap stars, showing strong broad blends at around λ4130 due to the Si II $\lambda\lambda$4128−30 doublet. Also present is the high-excitation Si II λ4200 line that is found only in the hotter Si stars. All four stars are clearly He weak and show rather weak Mg II λ4481 lines. Note the peculiarly Ca II K line profile in J020425.19+561142.4.

Among the Ap stars, the hot Si stars form a rather homogeneous group. They are characterized by strong Si II lines at λ3856, λ3862, and $\lambda\lambda$4128−30, the latter of which appear as a strong, flat-bottomed blend at LAMOST resolution. As this blend may be due to (or at least include contributions from) other ions beside Si II, it is imperative to check for the presence of the λ3856 and λ3862 lines to establish a Si peculiarity. In the red spectral region, the Si II lines at λ5041, $\lambda\lambda$5055/56, λ6347, and λ6371 are useful. Note the presence of the high-excitation Si II λ4200 line that is found only in the hotter Si stars. Most hot Si stars are noticeably He-weak, which led to their classification as A-type stars in the past, although most of them actually belong to spectral classes B8 and B9. They also often show weak Mg II λ4481 lines.

3.2 The SiCrEu stars

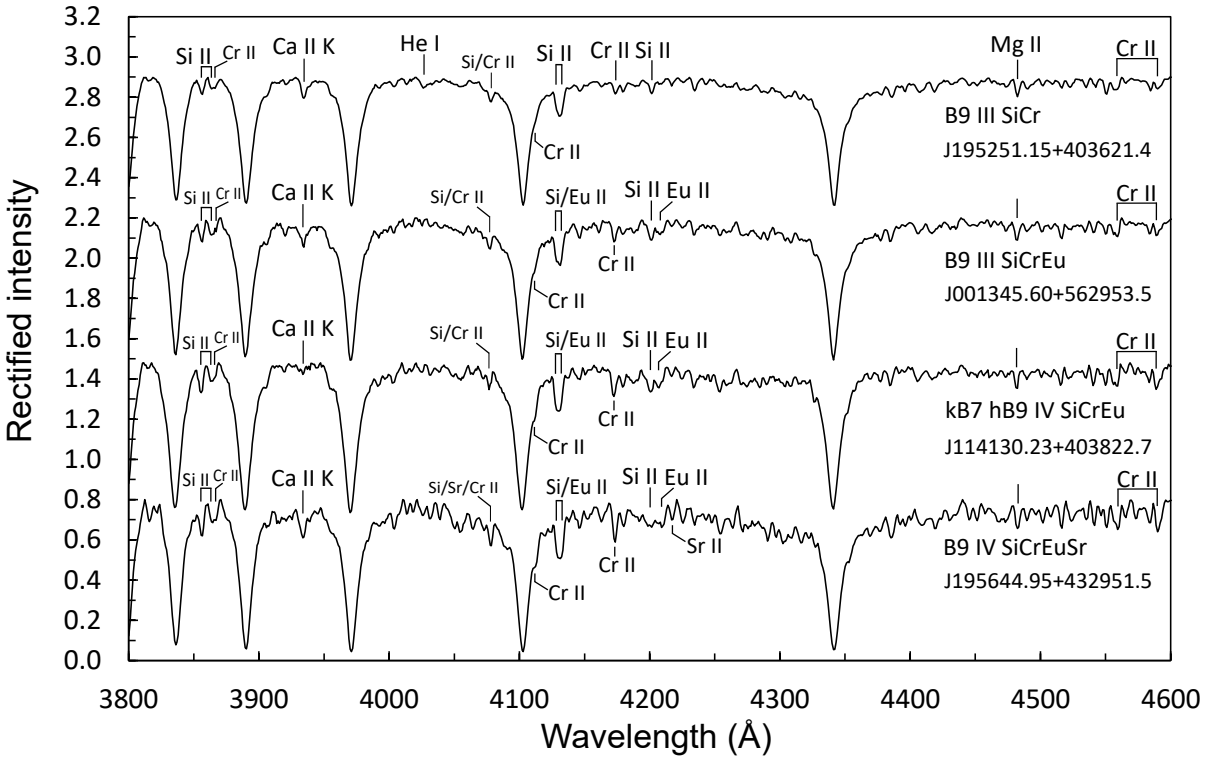

Figure 4: Four Ap stars that, in addition to strong Si II features (λ3856, λ3862, $\lambda\lambda$4128−30, and λ4200) show various other peculiarities. Note in particular the increasing strength of the Cr peculiarity (from top to bottom) and the very weak Ca II K line in J114130.23+403822.7.

Still at the hot end of the Ap star temperature distribution, one finds stars that, in addition to the Si II features of the hot Si stars (λ3856, λ3862, $\lambda\lambda$4128−30, and the high-excitation Si II line at λ4200), exhibit a mélange of other peculiarities. Most commonly observed in these objects is a Cr peculiarity, which, at LAMOST resolution, is readily identified by the strong Cr II lines at λ3866, λ4111, λ4172, and, to a lesser extent, also λ4559 and λ4588. Note that the λ4172 line, which is for example also enhanced in the Am stars (cf. Sect. 2), is blended with other ions (such as Fe II), and that λ4111 appears merely as a bump in the red wing of Hδ at this resolution. The importance of Eu II may be judged primarily from the λ4205 line, while the presence of a Sr peculiarity may be inferred from a peculiarly strong λ4216 line. All of the objects shown above show narrow hydrogen-line profiles that are best matched assuming luminosity classes III or IV (cf. Sect. 3.5).

3.3 The EuCrSr stars

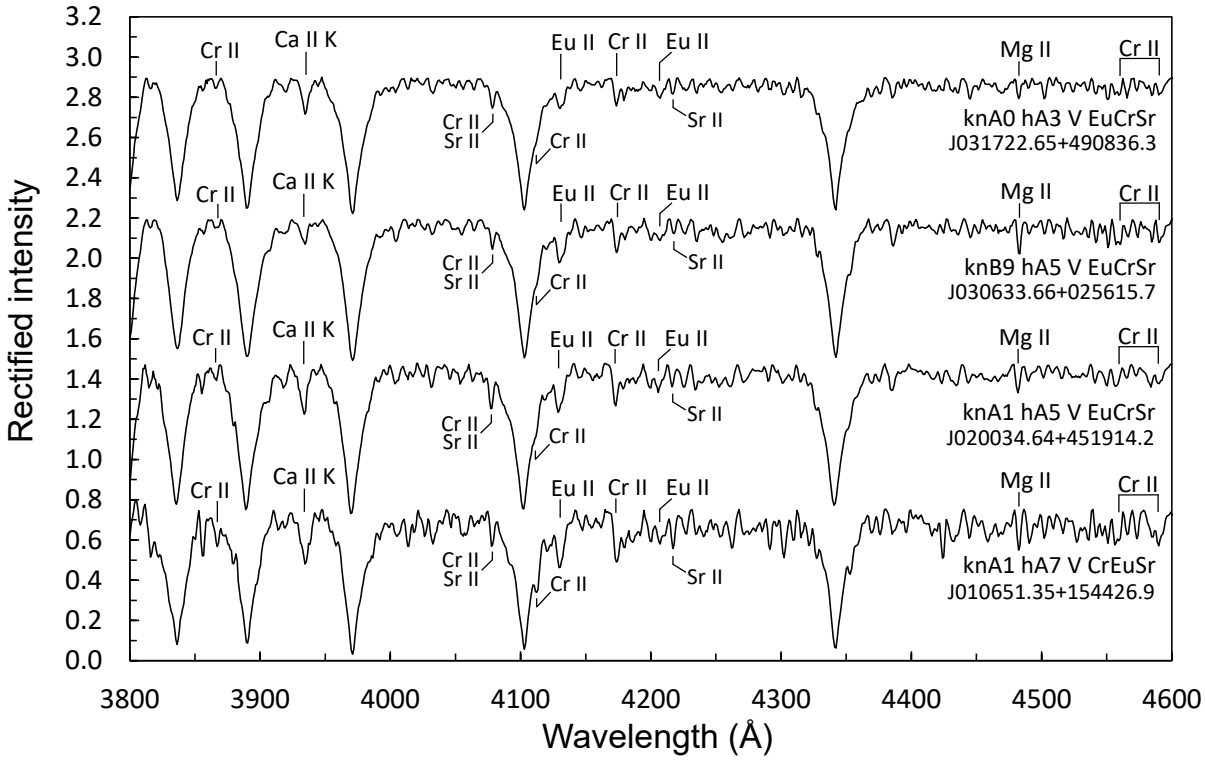

Figure 5: Four Ap stars of intermediate temperature, showing enhanced Cr II features (λ3866, λ4111, λ4172, λ4559, and λ4588) and strong Eu II (λ4130 and λ4205) and Sr II λ4216 lines. Here, the blends at λ4077 and λ4130 are dominated by Cr II+Sr II and Eu II, respectively. Note the diffuse (broad and shallow) Ca II K lines in all spectra.

With declining temperature, the contribution of Si II to the spectra of Ap stars generally decreases. In the spectra shown in Fig. 5, Si II, if present at all, plays only a minor part. At LAMOST resolution, what strikes the eye most in this group of stars is the enhanced Cr II lines and blends at λ3866, λ4111 (the bump in the red wing of Hδ), λ4172, λ4559, and λ4588, which are accompanied by strong Eu II lines at λ4130 and λ4205. The Sr II λ4216 line, so conspicuous in the spectra of the coolest Ap stars (Sect. 3.4), is still only moderately enhanced. In the illustrated spectra, the λ4077 blend is mostly due to Cr II and Sr II, while Eu II dominates the λ4130 blend. Luminosity classification is difficult for these objects because the sensitivity of the hydrogen-line profile to luminosity decreases for stars later than A3 (Gray and Garrison 1989b), and the usefulness of the blends usually employed for this purpose in late A-type stars, in particular the Fe/Ti II blends at $\lambda\lambda$4172−9 and λ4417, is diminished because of the peculiarity of the metallic-line spectrum. In fact, while the $\lambda\lambda$4172−9 blend appears stronger in J031722.65+490836.3 and J030633.66+025615.7 than in the corresponding standard stars, the Fe/Ti II blends at λ4395, λ4400, and λ4417 appear weaker, which reminds of the anomalous luminosity effect observed in the Am stars.

3.4 The cool SrCrEu stars

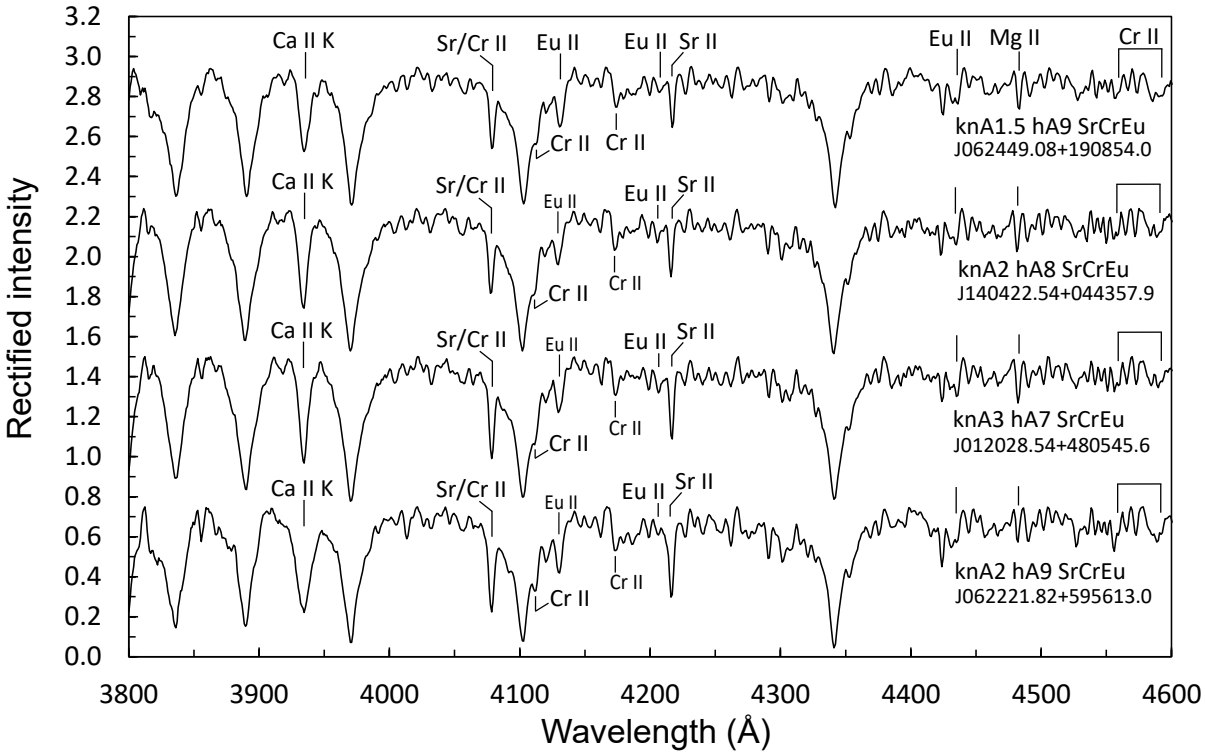

Figure 6: Four representative cool SrCrEu Ap stars, showing varying degrees of peculiarity. The most conspicuous features are the strong blend at λ4077, due to Cr II λ4076 and Sr II λ4077, as well as a very strong Sr II λ4216 line. Note also the contributions of Cr II at λ4111 (in the red wing of Hδ) and λ4172, and Eu II at λ4130, λ4205 and also λ4435. Note the diffuse (broad and shallow) Ca II K lines typical of these objects.

The SrCrEu Ap stars are situated at the cool end of the Ap star temperature distribution. Most of them are encountered around spectral type A5 or later. At LAMOST resolution, they are easily picked out by the strong line at λ4077, here due to Cr II λ4076 and Sr II λ4077, and the peculiarly strong Sr II λ4216 line. Several characteristic features due to Cr II and Eu II are also present, as indicated in Fig. 6. While Si peculiarities may span the whole effective temperature range of the Ap stars, in these cool objects, the λ4130 blend is usually dominated by Eu II and shows a different, round-bottomed morphology (cf. Sect. 3). In the four stars shown in Figure 6, there is no indication for a Si peculiarity, and λ4130 seems to be entirely due to Eu II. The cool SrCrEu Ap stars often show diffuse – that is, broad and shallow – Ca II K lines, which is acknowledged by the notation 'kn' in the spectral types provided in Fig. 6 and may be helpful to differentiate cool Ap stars from Am stars, which also show weak but rather narrow Ca II K lines (cf. Sect. 2).

3.5 Luminosity classification and the hydrogen-line profiles of Ap stars

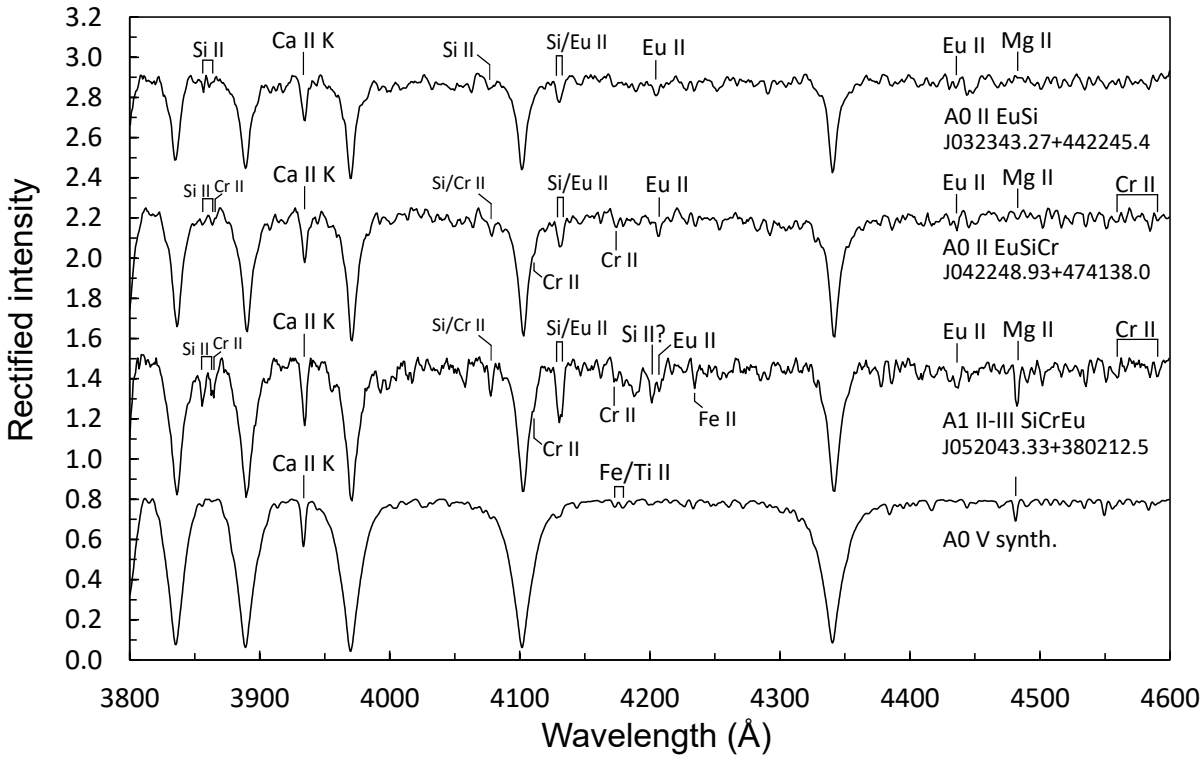

Figure 7: Three Ap stars showing peculiarly narrow hydrogen-line profiles. For comparison, a smoothed synthetic spectrum with $T_{\rm eff} = 9750\,{\rm K}$, $\log g = 4.0$, $[{\rm M/H}] = 0.0$, and a microturbulent velocity of 2 km/s (spectral type A0 V) is shown at the bottom. Note the very weak Mg II λ 4481 lines in J042248.93+474138.0 and, in particular, J032343.27+442245.4.

Particular caution is due when assigning a luminosity class to an Ap star. The utility of many traditional luminosity criteria, such as the strength of the Si II doublet at $\lambda\lambda$4128−30, the Fe/Ti II $\lambda\lambda$4172−9 and λ4417 blends, or the Fe II λ4233 and Mg II λ4481 lines, are severely compromised by the peculiarity of the metallic-line spectra. While most of the listed features tend to be overabundant in Ap stars, the λ4481 line often appears weak, leading to discrepant luminosities derived from different parts of the spectrum. Therefore, Ap stars are generally assigned a luminosity type based on the wings of their hydrogen lines. However, quite commonly, Ap stars exhibit peculiarly narrow hydrogen-line profiles that are best fit by the profiles of standards of luminosity class III (giants) or even higher luminosities. This is remarkable, because it has been well established that the vast majority of Ap stars are main-sequence objects (e.g. North 1993; Netopil et al. 2017) and should therefore belong to luminosity class V (dwarfs). While theory has yet to tackle this discrepancy, it seems conceivable that the strong magnetic fields have an impact on the atmospheric structure of these stars.

Fig. 7 illustrates three Ap stars with peculiarly narrow hydrogen-line profiles. Apart from the narrow hydrogen lines and strong Si II lines, the spectra of J032343.27+442245.4 and J042248.93+474138.0 lack other strong lines commonly associated with high luminosity. Note in particular the very weak Mg II λ4481 lines in these stars. J052043.33+380212.5, on the other hand, is a particular interesting case that also shows significantly enhanced lines of Fe II λ4233 and Mg II λ4481 and in the region

of the Fe/Ti II $\lambda\lambda$4172−9 blend, which support the high luminosity derived from the hydrogen-line profile. The strength of the Si II doublet $\lambda\lambda$4128−30, however, is much too strong even for a star of luminosity class II (bright giant).

Apart from this, the classifier needs to be aware that Ap stars may show other mild hydrogen-line profile peculiarities. In the more extreme Ap stars, the hydrogen-line profiles may be so peculiar that they do not match at any spectral type, which should be acknowledged by only indicating an approximate type denoted by a colon (Gray and Corbally 2009).

4 The HgMn stars

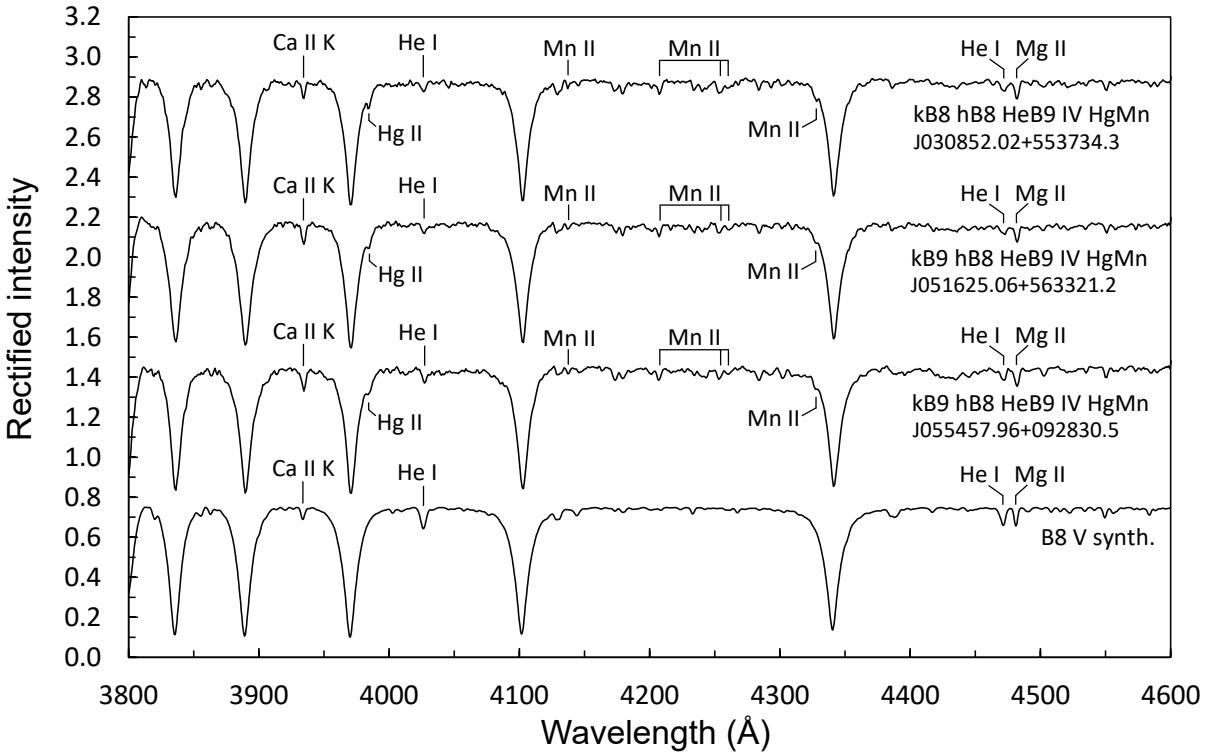

Figure 8: Three representative HgMn stars. The Hg II λ3984 line appears as just a bump in the red wing of the Hϵ line at this resolution. The most conspicuous Mn II features are located at λ4136, $\lambda\lambda$4252/9, and, in particular, λ4206. All shown objects have slightly weak He I lines. For comparison, a smoothed synthetic spectrum with $T_{\rm eff} = 12500$ K, $\log g = 4.0$, [M/H] = 0.0, and a microturbulent velocity of 2 km/s (spectral type B8 V) is provided at the bottom.

The HgMn/CP3 stars are B6−A0 objects characterized by strong overabundances of Hg and Mn (up to +6 dex and +3 dex over Solar, respectively). They are traditionally classified by the presence of Hg II and Mn II lines in the blue-violet spectral region. At LAMOST resolution, the Hg II λ3984 line appears as just a bump in the red wing of the Hϵ line. Prominent Mn II features are visible at λ4136, $\lambda\lambda$4252/9, and, in particular, λ4206. Be careful not to confuse the latter line with Eu II λ4205. Apart from that, a faint metallic-line spectrum is usually visible; note in particular the enhancements of the Fe/Ti II $\lambda\lambda$4172−9 blend traditionally employed in luminosity classification. All objects shown in Fig. 8 are noticeably He-weak. While, at high resolution, HgMn star spectra show numerous other peculiarities and often strikingly different abundance patterns from one star to the next, they appear as a rather uniform set of objects at LAMOST resolution. In general, their peculiarities appear much more subtle than what is observed in the Ap stars; nevertheless, in the temperature regime of the CP3 stars, the density of lines is rather low, and they can be readily picked out even at this low resolution. A good summary of the observed peculiarities in CP3 stars is provided by Ghazaryan and Alecian (2016).

5 The He-peculiar stars

5.1 The He-weak stars

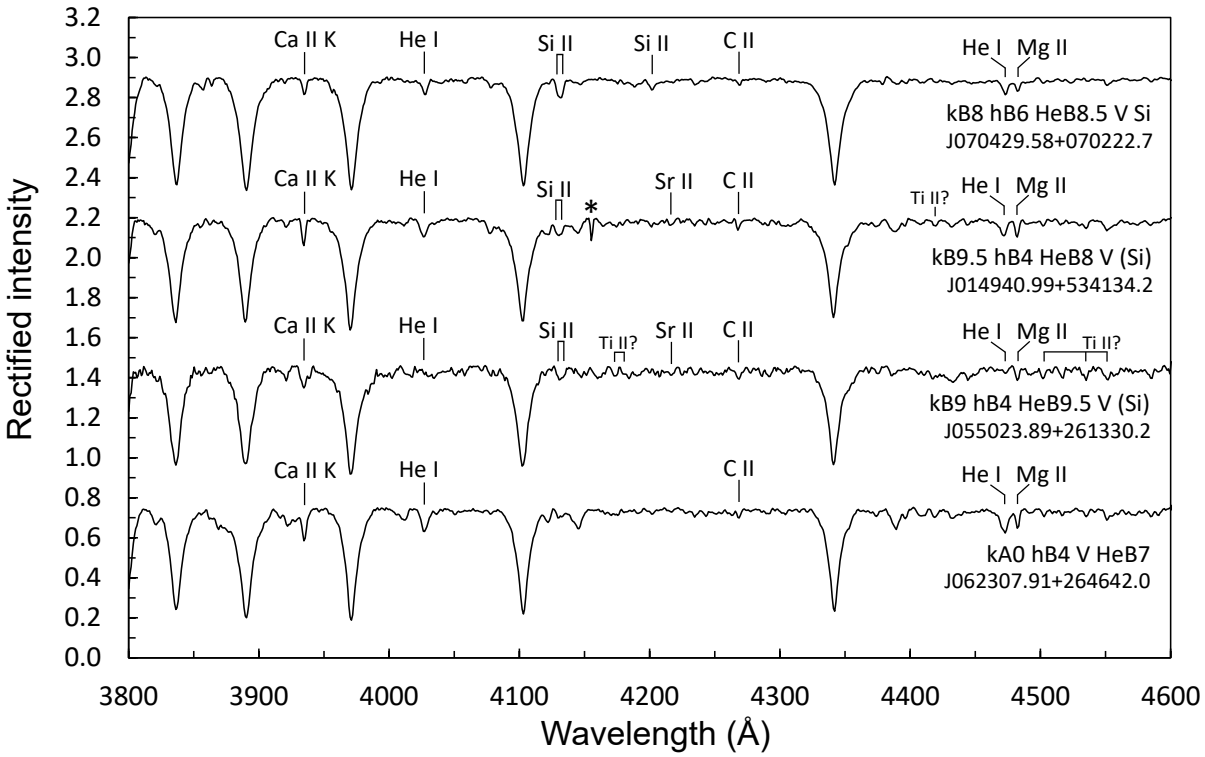

Figure 9: Four representative He-weak stars. The He-weak nature of all objects is directly obvious. Note the strong C II λ4267 lines and the peculiar, triangular-shaped He I line profiles of, in particular, J062307.91+264642.0. The asterisk marks a glitch in the spectrum of J014940.99+534134.2.

The He-weak/CP4 stars are B-type stars (usually B3 and later) with unusually weak He I lines for the spectral type derived from the hydrogen-line profile. Because of this, a spectral type based on the strength of the He I lines is usually specified for these objects (Osawa 1965; Garrison and Gray 1994). Further characteristics of this group (which may or may not be all present in a given object) are rather prominent metallic lines, unusual (mostly broad and triangular) He I line profiles (noticeable, in particular, in the λ4471 line), and lines of C II λ4267 and Si III λ4552. Three different subgroups have been described: the **Si stars**, which show enhanced lines of Si II (but at higher temperatures than the Ap Si stars, which are also often He weak); the **PGa stars**, characterized by peculiarly strong lines of P and Ga; and the **SrTi stars**, which show enhanced lines of Sr and Ti. While these subclasses can be identified in high S/N classification spectra with resolutions better than 2 Å (Gray and Corbally 2009), the present author has found it difficult to assign them at LAMOST resolution (∼2.5 Å). All spectra illustrated in Fig. 9 have noticeably weak He I lines but a rather strong λ4267 line, which corroborates the temperature types based on the hydrogen-line profile. While J070429.58+070222.7 is certainly a He-weak star of the Si type, things are less clear in the case of the other objects, all of which show prominent metallic lines. J014940.99+534134.2 and J055023.89+261330.2 may be SrTi stars but also show marginally enhanced Si II $\lambda\lambda$4128−30 doublets. J062307.91+264642.0 does not fit any of the standard subclasses.

5.2 The He-rich stars

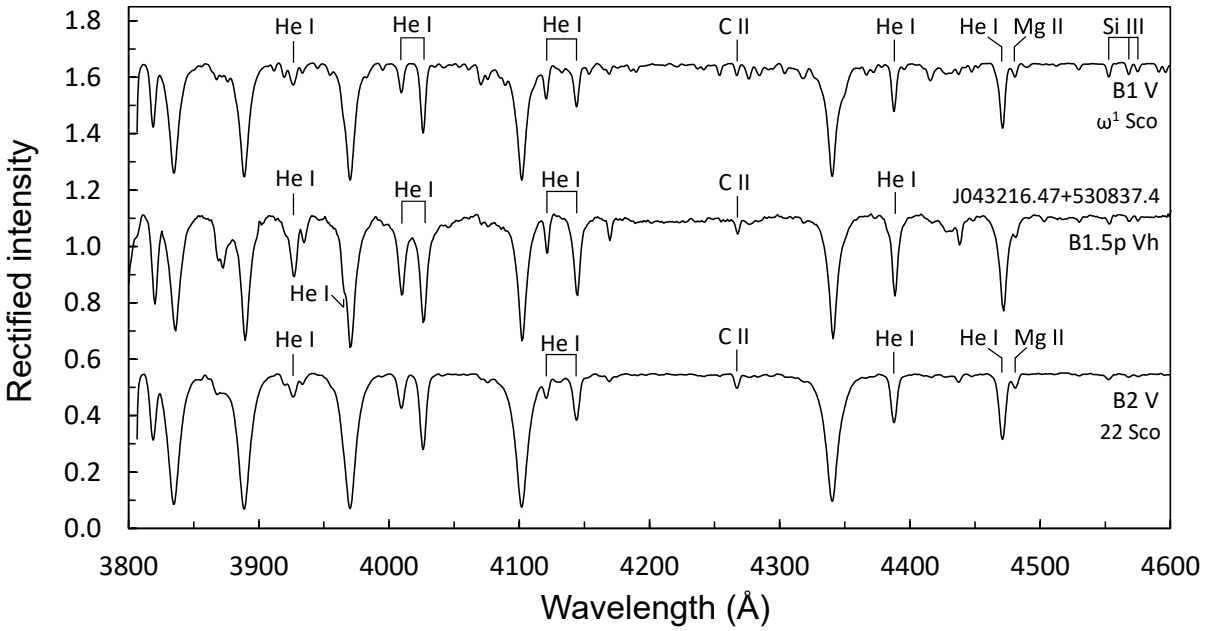

Figure 10: The spectrum of the He-rich star J043216.47+530837.4, compared with, respectively, the spectra of the B1 V and B2 V standards ω^1 Sco and 22 Sco, which were taken from the *libr18_225* collection of standard spectra that contains spectra smoothed to a resolution of 2.25 Å.

He-rich stars are a rare group of CP stars and encountered among stars of spectral type B3 and earlier, the best-known examples being σ Ori E and δ Ori C. As their name implies, the most obvious feature of the He-rich stars is the presence of peculiarly strong lines of He I in their spectra. As is obvious from Fig. 10, the hydrogen-line type of J043216.47+530837.4 appears to be intermediate between B1 V and B2 V, while the lines of He I are rather broad and extraordinarily strong. It has thus been given a classification of B1.5p Vh, with the succeeding letter "h" indicating the He-strong nature of this star. Other peculiarities, such as a strong C II λ4267 line and weak Si III and Si IV lines, may be present (Gray and Corbally 2009).

6 The λ Bootis stars

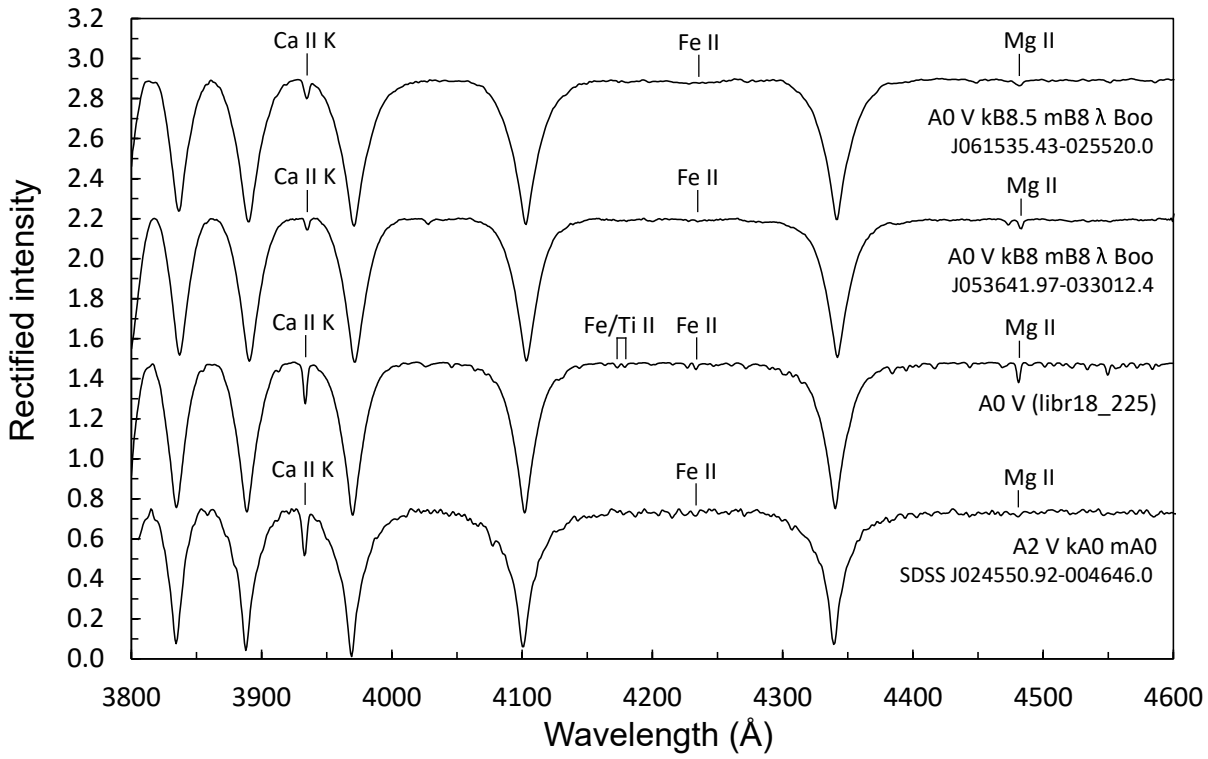

Figure 11: Two early λ Bootis stars (upper two spectra), compared with an A0 V standard star spectrum taken from the *libr18_225* collection, and the SDSS spectrum of a BHB star candidate (bottom spectrum). Note the very weak Mg II λ4481 lines in the three CP stars.

The most obvious characteristic of the λ Bootis stars, which are encountered in the spectral type range from B9.5 to F0 (or even later; Gray and Corbally 2009), is their metal-weak nature, that is, the metallic-line spectrum and the Ca II K line appear significantly weak for the temperature type as determined from the hydrogen lines. λ Bootis stars furthermore show weak Mg II λ4481 lines and a broad hydrogen-line profile indicative of a main-sequence object. Apart from these features, at LAMOST resolution, the spectra of early λ Bootis stars appear nearly featureless (Fig. 11; upper two spectra) and are readily picked out by eye. However, at this resolution, it is difficult to distinguish λ Bootis stars from certain groups of metal-weak population II stars, such as for example A-type blue horizontal-branch (BHB) stars, which also appear noticeably metal-weak and show notoriously weak λ4481 lines. As an example, the bottom spectrum in Fig. 11 illustrates the spectrum of the BHB star candidate SDSS J024550.92-004646.0, which shows a particularly weak λ4481 line. Space velocity information is important to distinguish these groups of stars; useful spectroscopic criteria for their differentiation are provided in Section 5.6.1 of Gray and Corbally (2009). In general, in the classification of λ Bootis stars, the spectral types derived from the Ca II K line, the hydrogen lines, and the strength of the metallic lines are provided, similar to the notation used for the Am stars (cf. Sect. 2). To avoid confusion, the suffix "λ Boo" is added (cf. the classifications provided in Fig. 11). Detailed information on the classification of λ Bootis stars has been provided by Gray (1988).

Acknowledgments

Guoshoujing Telescope (the Large Sky Area Multi-Object Fiber Spectroscopic Telescope LAMOST) is a National Major Scientific Project built by the Chinese Academy of Sciences. Funding for the project has been provided by the National Development and Reform Commission. LAMOST is operated and managed by the National Astronomical Observatories, Chinese Academy of Sciences. This research has made use of the SIMBAD database and the VizieR catalogue access tool (DOI : 10.26093/cds/vizier), operated at CDS, Strasbourg, France. The original description of the VizieR service was published in 2000, A&AS 143, 23.

7 References

F. Castelli and R. L. Kurucz. New Grids of ATLAS9 Model Atmospheres. In N. Piskunov, W. W. Weiss, and D. F. Gray, editors, *Modelling of Stellar Atmospheres*, volume 210 of *IAU Symposium*, page A20, Jan 2003.

Xiang-Qun Cui, Yong-Heng Zhao, Yao-Quan Chu, Guo-Ping Li, Qi Li, Li-Ping Zhang, Hong-Jun Su, Zheng-Qiu Yao, Ya-Nan Wang, Xiao-Zheng Xing, Xin-Nan Li, Yong-Tian Zhu, Gang Wang, Bo-Zhong Gu, A-Li Luo, Xin-Qi Xu, Zhen-Chao Zhang, Gen-Rong Liu, Hao-Tong Zhang, De-Hua Yang, Shu-Yun Cao, Hai-Yuan Chen, Jian-Jun Chen, Kun-Xin Chen, Ying Chen, Jia-Ru Chu, Lei Feng, Xue-Fei Gong, Yong-Hui Hou, Hong-Zhuan Hu, Ning-Sheng Hu, Zhong-Wen Hu, Lei Jia, Fang-Hua Jiang, Xiang Jiang, Zi-Bo Jiang, Ge Jin, Ai-Hua Li, Yan Li, Ye-Ping Li, Guan-Qun Liu, Zhi-Gang Liu, Wen-Zhi Lu, Yin-Dun Mao, Li Men, Yong-Jun Qi, Zhao-Xiang Qi, Huo-Ming Shi, Zheng-Hong Tang, Qing-Sheng Tao, Da-Qi Wang, Dan Wang, Guo-Min Wang, Hai Wang, Jia-Ning Wang, Jian Wang, Jian-Ling Wang, Jian-Ping Wang, Lei Wang, Shu-Qing Wang, You Wang, Yue-Fei Wang, Ling-Zhe Xu, Yan Xu, Shi-Hai Yang, Yong Yu, Hui Yuan, Xiang-Yan Yuan, Chao Zhai, Jing Zhang, Yan-Xia Zhang, Yong Zhang, Ming Zhao, Fang Zhou, Guo-Hua Zhou, Jie Zhu, and Si-Cheng Zou. The large sky area multi-object fiber spectroscopic telescope (lamost). *Research in Astronomy and Astrophysics*, 12(9):1197, 2012. URL http://stacks.iop.org/1674-4527/12/i=9/a=003.

R. F. Garrison and R. O. Gray. The Late B-Type Stars: Refined MK Classification, Confrontation With Stromgren Photometry, And The Effects of Rotation. *Astronomical Journal*, 107:1556, April 1994. doi: 10.1086/116967.

S. Ghazaryan and G. Alecian. Statistical analysis from recent abundance determinations in HgMn stars. *MNRAS*, 460:1912–1922, August 2016. doi: 10.1093/mnras/stw911.

R. O. Gray. The Spectral Classification of the Lambda Bootis Stars. *Astronomical Journal*, 95: 220, January 1988. doi: 10.1086/114631.

R. O. Gray and C. J. Corbally. The Calibration of MK Spectral Classes Using Spectral Synthesis. I. The Effective Temperature Calibration of Dwarf Stars. *Astronomical Journal*, 107:742, Feb 1994. doi: 10.1086/116893.

R. O. Gray and C. J. Corbally. *Stellar Spectral Classification*. Princeton, NJ: Princeton Univ. Press, 2009.

R. O. Gray and R. F. Garrison. The early A type stars - Refined MK classification, confrontation with Stroemgren photometry, and the effects of rotation. *The Astrophysical Journal Supplement Series*, 65:581–602, December 1987. doi: 10.1086/191237.

R. O. Gray and R. F. Garrison. The early F-type stars - Refined classification, confrontation with Stromgren photometry, and the effects of rotation. *The Astrophysical Journal Supplement Series*, 69:301–321, February 1989a. doi: 10.1086/191315.

R. O. Gray and R. F. Garrison. The late A-type stars - Refined MK classification, confrontation with Stromgren photometry, and the effects of rotation. *The Astrophysical Journal Supplement Series*, 70:623–636, July 1989b. doi: 10.1086/191349.

S. Hümmerich, E. Paunzen, and K. Bernhard. A plethora of new, magnetic chemically peculiar stars from LAMOST DR4. *Astronomy & Astrophysics*, 640:A40, August 2020. doi: 10.1051/0004-6361/202037750.

Carlos Jaschek and Mercedes Jaschek. *The classification of stars*. Cambridge: University Press, 1987.

A. L. Luo, Y. H. Zhao, G. Zhao, and et al. VizieR Online Data Catalog: LAMOST DR4 catalogs (Luo+, 2018). *VizieR Online Data Catalog*, art. V/153, August 2018.

W. W. Morgan, Helmut A. Abt, and J. W. Tapscott. *Revised MK Spectral Atlas for stars earlier than the sun*. Williams Bay: Yerkes Observatory, and Tucson: Kitt Peak National Observatory, 1978.

Simon J. Murphy, Christopher J. Corbally, Richard O. Gray, Kwang-Ping Cheng, James E. Neff, Chris Koen, Charles A. Kuehn, Ian Newsome, and Quinlin Riggs. An Evaluation of the Membership Probability of 212 λ Boo Stars. I. A Catalogue. *Publications of the Astronomical Society of Australia*, 32:43, October 2015. doi: 10.1017/pasa.2015.34.

Martin Netopil, Ernst Paunzen, Stefan Hümmerich, and Klaus Bernhard. An investigation of the rotational properties of magnetic chemically peculiar stars. *MNRAS*, 468(3):2745–2756, July 2017. doi: 10.1093/mnras/stx674.

P. North. Chemically Peculiar Stars in Clusters - Upper and Lower Age Limits of Cp-Stars. In M. M. Dworetsky, F. Castelli, and R. Faraggiana, editors, *IAU Colloq. 138: Peculiar versus Normal Phenomena in A-type and Related Stars*, volume 44 of *Astronomical Society of the Pacific Conference Series*, page 577, January 1993.

Kiyoteru Osawa. Spectral classification and three-color photometry of A-type peculiar stars. *Annals of the Tokyo Astronomical Observatory*, 9(3):121–144, January 1965.

E. Paunzen, S. Hümmerich, and K. Bernhard. New mercury-manganese stars and candidates from LAMOST DR4. *Astronomy & Astrophysics*, 645:A34, January 2021. doi: 10.1051/0004-6361/202038847.

G. W. Preston. The chemically peculiar stars of the upper main sequence. *Annual Rev. Astron. Astrophys*, 12:257–277, 1974. doi: 10.1146/annurev.aa.12.090174.001353.

Antoni Przybylski. HD 101065 – a G0 Star with High Metal Content. *Nature*, 189(4766):739, March 1961. doi: 10.1038/189739a0.

Li Qin, A. Li Luo, Wen Hou, Yin-Bi Li, Shuo Zhang, Rui Wang, Li-Li Wang, Xiao Kong, and Jin-Shu Han. Metallic-line Stars Identified from Low-resolution Spectra of LAMOST DR5. *The Astrophysical Journal Supplement Series*, 242(2):13, June 2019. doi: 10.3847/1538-4365/ab17d8.

Sidney C. Wolff. *The A-stars : problems and perspectives*. Paris: Centre National de la Recherche Scientifique (CNRS), Washington: NASA, 1983. Monograph Series on Nonthermal phenomena in Stellar Atmospheres.

Gang Zhao, Yong-Heng Zhao, Yao-Quan Chu, Yi-Peng Jing, and Li-Cai Deng. Lamost spectral survey – an overview. *Research in Astronomy and Astrophysics*, 12(7):723, 2012. URL http://stacks.iop.org/1674-4527/12/i=7/a=002.

Appendix

Table 1 contains conventional identifiers for all stars used in this work, the sources, from which these objects have been gleaned, and download links for all spectra depicted herein. For each object, there are two download links. The first link accesses the original LAMOST DR4 spectrum in tsv ("tab separated values") format as provided in the VizieR online catalogue (Luo et al. 2018), the second link provides the spectrum in rectified and normalized flux, which has been the basis for all figures depicted herein. Please note that the normalization has been performed manually by the present author and may not represent the most optimal solution and that some of the noisier spectra were slightly smoothed.

Table 1: Alternative identifiers, sources and download links for all CP stars used in this study. The columns denote: (1) LAMOST identifier. (2) Alternativ identifier. (3) CP subgroup. (4) Source. (5) Download link for the original DR4 spectrum (tsv format via VizieR). (6) Download link for the spectrum in normalized and rectified flux.

LAMOST_ID	alt_ID	CP_subgroup	Source	SP_orig	SP_norm
J062107.99+353726.2	TYC 2429-564-1	Am	Qin et al. (2019)	VizieR	link2
J181058.85+144337.1	TYC 1021-464-1	Am	Qin et al. (2019)	VizieR	link2
J190045.36+443850.2	TYC 3132-1242-1	Am	Qin et al. (2019)	VizieR	link2
J003312.88+543141.3	TYC 3658-79-1	Ap(Si)	Hümmerich et al. (2020)	VizieR	link2
J020425.19+561142.4	TYC 3689-1567-1	Ap(Si)	Hümmerich et al. (2020)	VizieR	link2
J060809.53+240945.0	HD 252026	Ap(Si)	Hümmerich et al. (2020)	VizieR	link2
J203337.82+480113.3	TYC 3577-1410-1	Ap(Si)	Hümmerich et al. (2020)	VizieR	link2
J195251.15+403621.4	HD 226339	Ap(SiCrEu)	Hümmerich et al. (2020)	VizieR	link2
J001345.60+562953.5	TYC 3661-1153-1	Ap(SiCrEu)	Hümmerich et al. (2020)	VizieR	link2
J114130.23+403822.7	TYC 3014-2468-1	Ap(SiCrEu)	Hümmerich et al. (2020)	VizieR	link2
J195644.95+432951.5	TYC 3149-1303-1	Ap(SiCrEu)	Hümmerich et al. (2020)	VizieR	link2
J031722.65+490836.3	TYC 3319-464-1	Ap(EuCrSr)	Hümmerich et al. (2020)	VizieR	link2
J030633.66+025615.7	TYC 58-1131-1	Ap(EuCrSr)	Hümmerich et al. (2020)	VizieR	link2
J020034.64+451914.2	TYC 3280-1768-1	Ap(EuCrSr)	Hümmerich et al. (2020)	VizieR	link2
J010651.35+154426.9	HD 6590	Ap(EuCrSr)	Hümmerich et al. (2020)	VizieR	link2
J062449.08+190854.0	GSC 01336-00888	Ap(SrCrEu)	Hümmerich et al. (2020)	VizieR	link2
J140422.54+044357.9	TYC 319-461-1	Ap(SrCrEu)	Hümmerich et al. (2020)	VizieR	link2
J012028.54+480545.6	TYC 3269-867-1	Ap(SrCrEu)	Hümmerich et al. (2020)	VizieR	link2
J062221.82+595613.0	TYC 3776-269-1	Ap(SrCrEu)	Hümmerich et al. (2020)	VizieR	link2
J032343.27+442245.4	GSC 02873-00829	Ap(H_profile)	Hümmerich et al. (2020)	VizieR	link2
J042248.93+474138.0	TYC 3333-1433-1	Ap(H_profile)	Hümmerich et al. (2020)	VizieR	link2
J052043.33+380212.5	GSC 02909-01224	Ap(H_profile)	Hümmerich et al. (2020)	VizieR	link2
J030852.02+553734.3	TYC 3706-249-1	HgMn	Paunzen et al. (2021)	VizieR	link2
J051625.06+563321.2	TYC 3743-51-1	HgMn	Paunzen et al. (2021)	VizieR	link2
J055457.96+092830.5	HD 249170	HgMn	Paunzen et al. (2021)	VizieR	link2
J070429.58+070222.7	TYC 174-585-1	He-wk	unpublished	VizieR	link2
J014940.99+534134.2	TYC 3684-1139-1	He-wk	Hümmerich et al. (2020)	VizieR	link2
J055023.89+261330.2	TYC 1866-861-1	He-wk	Hümmerich et al. (2020)	VizieR	link2
J062307.91+264642.0	UCAC4 584-028577	He-wk	Hümmerich et al. (2020)	VizieR	link2
J043216.47+530837.4	BD+52 840	He-st	unpublished	VizieR	link2
J061535.43-025520.0	HD 294806	λ Boo	unpublished	VizieR	link2
J053641.97-033012.4	HD 294253	λ Boo	Murphy et al. (2015)	VizieR	link2